actuators

MDPI

Article

Target Tracking and Circumnavigation Control for Multi-Unmanned Aerial Vehicle Systems Using Bearing Measurements

Zican Zhou [1], Jiangping Hu [1,2,*], Bo Chen [3], Xixi Shen [1] and Bin Meng [4]

[1] School of Automation Engineering, University of Electronic Science and Technology of China, Chengdu 611731, China; zhouzc@std.uestc.edu.cn (Z.Z.); xixishen@std.uestc.edu.cn (X.S.)
[2] Yangtze Delta Region Institute (Huzhou), University of Electronic Science and Technology of China, Huzhou 313000, China
[3] School of Science, Chongqing University of Posts and Telecommunications, Chongqing 400065, China; chenbo@cqupt.edu.cn
[4] Beijing Institute of Control Engineering, Beijing 100080, China; mengb@amss.ac.cn
* Correspondence: hujp@uestc.edu.cn

Abstract: This paper addresses the problem of target tracking and circumnavigation control for a bearing-only multi-Unmanned Aerial Vehicle (UAV) system. First, using the bearing measurements, an adaptive algorithm in the form of a Proportional Integral (PI) controller is developed to estimate the target state. Subsequently, a distributed circumnavigation control protocol is established to evenly encircle the target. Then, we use the local information from each UAV in the network to calculate the relative position of the target, and further enhance the accuracy of estimation and circumnavigation algorithms by employing a Kalman filter. Finally, numerical simulation experiments are conducted to validate the effectiveness of the proposed tracking control algorithm.

Keywords: multi-UAV system; bearing measurement; target tracking; circumnavigation control; Kalman filtering

check for updates

Citation: Zhou, Z.; Hu, J.; Chen, B.; Shen, X.; Meng, B. Target Tracking and Circumnavigation Control for Multi-Unmanned Aerial Vehicle Systems Using Bearing Measurements. *Actuators* **2024**, *13*, 323. https://doi.org/10.3390/act13090323

Academic Editors: Bailing Tian, Hongyang Bai and Lihui Wang

Received: 12 July 2024
Revised: 18 August 2024
Accepted: 23 August 2024
Published: 25 August 2024

Copyright: © 2024 by the authors. Licensee MDPI, Basel, Switzerland. This article is an open access article distributed under the terms and conditions of the Creative Commons Attribution (CC BY) license (https://creativecommons.org/licenses/by/4.0/).

1. Introduction

In recent years, the problem of target tracking and circumnavigation control has garnered significant research attention due to its wide range of applications. These applications include satellite formation flying, dynamic encirclement by multiple Unmanned Aerial Vehicles (UAVs), and cooperative surrounding missions involving multiple vessels [1–4]. In general, the position of the target is initially unavailable for the agents, thus requiring an estimator to estimate the target state [5,6]. Particularly, in some military scenarios, to maintain radio silence, the passive target locating and tracking techniques, which uses only the bearings measured by camera, has become a hot research field [7–9].

Researchers commonly utilized target bearing data to estimate unknown states and update control algorithms, merging localization and circumnavigation control. This strategy enhances system performance via environmental observation and recognition, thus addressing a dual problem [10]. In early studies [11–13], the method employing an orthogonal projection matrix was introduced to handle unit bearing vectors, enabling an agent to estimate the target position and accomplish the circumnavigation mission of static or slowly moving targets. In [14], this approach has been extended to multi-agent systems for circumnavigation control of multiple static targets. In [15], the authors established a condition to ensure a safe distance between agents and targets, preventing agents from entering the proximity of targets during circumnavigation. In [16,17], corresponding control frameworks are proposed to enable the estimator's application to a single or multiple UAVs for target encirclement. Later, the authors of [18–20] employed the linear filter and finite-time stability theory to enhance the convergence rate of the estimator. This enhancement allows

the multi-agent system to rapidly enclose the targets. For multi-drone motion planning, especially for large drone teams, studying collision avoidance strategies between drones is fundamental and crucial [21,22]. Researchers in [23–25] further investigated the discrete-time and communication-free circumnavigation control problem, incorporating collision avoidance among agents to enhance the system's applicability in real-world scenarios.

However, the aforesaid consequences [11–20,23–25] heavily rely on GPS devices for agents to acquire real-time global position data, which is crucial for target estimation. Yet, in hostile environments, GPS signals are susceptible to disruption or attacks, potentially compromising target tracking effectiveness [26]. Addressing this challenge, researchers proposed the concept of distributed bearing-only formation control [27–29]. Within this framework, agents only need to measure the relative bearings between each other, without reliance on GPS information. Target state estimation is often integrated with multi-agent formation control, utilizing bearing measurements for more sophisticated target tracking and cooperative motion. For instance, in [30], the bearing rigidity theory and a rotation matrix were used to establish a time-varying formation for encircling a moving target. Additionally, a dynamic compensation approach in [31] modified traditional target estimators to calculate relative target positions without global information. Building on this, refined target estimators in [32,33] relaxed the initial condition requirements, enabling adept navigation around one or multiple targets in circular or convex trajectories. Furthermore, the researchers in [34,35] analyzed target tracking and circumnavigation within GPS-free systems involving multiple vessels and second-order agents, proposing tailored algorithms for specific dynamic models. Despite their effectiveness, these estimation and control strategies heavily rely on precise sensor data, and may not adequately address high-speed target scenarios. Addressing these limitations is essential for enhancing performance and expanding applicability.

Motivated by the above discussion, this paper is devoted to solving the target tracking and circumnavigation control problem for a moving target within bearing-based networked multi-UAV systems. The main contributions of this paper are presented as follows:

(1) A distributed target estimation algorithm and a circumnavigation control protocol are designed by using bearing measurements of the target. In contrast to the proportional (P) estimator used in [11–20,23–25,29–33], we introduce a PI control method to develop the estimator, which significantly enhances its robustness. It can be proven that the algorithm converges to a bounded range near the true value. Moreover, in comparison with [11–20,23–25], we take into account practical communication range restrictions and employ dynamic compensation to enable the system to track and encircle the target in a GPS-denied environment.

(2) A Kalman filter approach is applied to improve the accuracy of target estimation and circumnavigation control. Each UAV in the system utilizes local information, including relative bearing and velocity data from neighbors, to calculate measurements of the target's relative position. These measurements are then incorporated into a Kalman filter for target state estimation. This approach enhances circumnavigation tracking precision, enabling successful tracking of the dynamic target within the system. Compared to previous methods [11–20,23–25,28–35], our approach leverages effective communication and collaboration among agents to achieve superior target localization and circumnavigation performance, especially in high-speed target scenarios.

The rest of this paper is structured below. In Section 2, the problem to be investigated and necessary preliminaries are given. In Section 3, the distributed target-state estimator and circumnavigation control algorithm are designed. In Section 4, the precise estimator and modified circumnavigation control strategy by Kalman filtering method are developed. In Section 5, simulation results are presented. Finally, conclusions are summarized in Section 6.

2. Preliminaries and Problem Statement

2.1. Notations

All vectors in $\mathbb{R}^n$ are n dimensional column vectors. For a given vector or matrix X, X^{T} denotes its transposition. I_n is an identity matrix with n dimensions, and when n is 2, it is simply written as I. For a unit vector $\varphi \in \mathbb{R}^n$, let $P_\varphi = I_n - \varphi\varphi^{\mathrm{T}}$ be the corresponding projection matrix and $\bar{\varphi} \in \mathbb{R}^n$ be the unit vector perpendicular to φ, obtained by $\frac{\pi}{2}$ clockwise rotation of φ. Let $\|\cdot\|$ be the Euclidean norm or the spectral norm of a matrix. The symbol $\otimes$ represents the Kronecker product. For a random variable Y, $E[Y]$ represents its expectation. For the convenience of expression, if there is no special description, the symbol (t) is omitted in this paper.

2.2. Problem Statement

In this paper, we consider a multi-agent system consisting of n fixed-wing UAVs i, $i \in \Omega = \{1, \cdots, n\}$, flying at different altitudes. Using the feedback linearization method, each UAV can be described as a single integrator model [16,36]:

$$\dot{p}_i = u_i, \quad i \in \Omega, \tag{1}$$

where $p_i \in \mathbb{R}^2$ and $u_i \in \mathbb{R}^2$ represent the position and the control input of UAV i. The UAVs are required to locate and circumnavigate a moving target with an unknown position $p_0 \in \mathbb{R}^2$. We assume that the trajectory of the target p_0 is differential, and there exists a positive finite constant ε such that for $t \geq 0$, $\| \dot{p}_0 \| \leq \varepsilon$.

We suppose that the UAVs operate in a GPS-denied environment. As a result, each UAV cannot acquire its own global position, and instead only maintains a local frame $\sum^i$ with the origin at p_0, while relying on the compass to ensure that its orientation aligns with the global frame $\sum^g$. In $\sum^i$, we define p_{i0} as the relative position between the target and UAV i, which can be obtained as $p_{i0} = p_0 - p_i$. Each UAV is equipped with a camera to measure its bearing relative to the target, and the bearing can be represented as the unit vector φ_{i0} in the direction $p_0 - p_i$:

$$\varphi_{i0} = \frac{p_{i0}}{\| p_{i0} \|}, \quad i \in \Omega. \tag{2}$$

When measuring bearings of the target, we use the correlated double sampling method to eliminate sensor measurement noise. Moreover, the UAVs has a communication radius $\rho > 0$, within which they can the exchange bearing information and their own velocity data. Let N_i represent the set of neighboring UAVs within the communication range of UAV i, defined as $N_i = \{j \in \{1, \cdots, n\}/\{i\} : \| p_j - p_i \| \leq \rho\}$. Let $\Delta_{ij} \geq 0$ denote the counterclockwise angle from φ_{i0} to φ_{j0}. The UAV $j \in N_i$ that achieves the minimum value of Δ_{ij} will be designated as v_i. Furthermore, if N_i is nonempty, we let $\Delta_i = \Delta_{i,v_i}$, $p_{i,v_i} = p_{v_i} - p_i$, $\varphi_{i,v_i} = \frac{p_{i,v_i}}{\|p_{i,v_i}\|}$, and $\theta_{v_i,0}$ represent the angle between the edge from UAV v_i to the target and the edge from UAV v_i to UAV i, as depicted in Figure 1. Note that when N_i is empty, we have $\Delta_i = 0$; and when $\varphi_{i0} = \varphi_{v_i,0}$, we let $\Delta_i(t) = 0$ if $\Delta_i(t^-) = 0^+$, $\Delta_i(t) = 2\pi$ if $\Delta_i(t^-) = 2\pi^-$.

Since the UAVs cannot directly obtain the accurate relative position of the target, UAV i needs to maintain a real-time estimate $\hat{p}_{i0}$ in its local frame $\sum^i$. Thus, the estimation error of the relative position of the target by UAV i is

$$\tilde{p}_{i0} = \hat{p}_{i0} - p_{i0}, \quad i \in \Omega. \tag{3}$$

Our research focuses on developing a localization algorithm and a control strategy for the multi-UAV system. The goal is to accurately and efficiently locate and circumnavigate a moving target using bearing measurements. We aim to achieve circumnavigation tracking while ensuring a uniform distribution of UAVs along the surrounding orbit. In terms of the

control objective, we will formally present the problem statement for the target tracking and circumnavigation control problem.

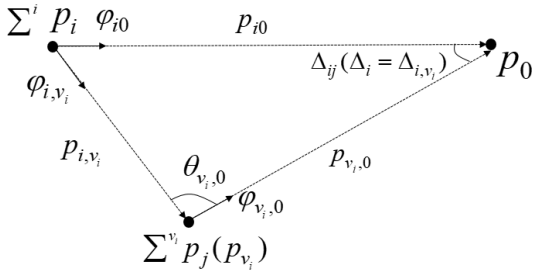


Figure 1. Illustration of the case that when $j = v_i$, the geometric relationship between bearings and relative positions of the target and UAVs.

Problem 1 (Target tracking and circumnavigation control problem)**.** *With bearing-only measurements to the target, for each UAV i, design an estimator and a controller such that the following objectives can be achieved:*

$$\lim_{t\to\infty} \| \tilde{p}_{i0} \| \leq \mathrm{U}_0, \quad i \in \Omega, \tag{4}$$

$$\lim_{t\to\infty} \left| D_i - D^* \right| \leq \mathrm{U}_1, \quad i \in \Omega, \tag{5}$$

$$\lim_{t\to\infty} |\Delta_i - \frac{2\pi}{n}| \leq \mathrm{U}_2, \quad i \in \Omega, \tag{6}$$

where U_0, U_1 *and* U_2 *are nonnegative constants associated with* ε, $D_i = \| p_{i0} \|$ *denotes the relative distance between UAV i and the target. The parameter* D^* *represents the desired circumnavigation radius, which is a prescribed positive value.*

2.3. Technical Lemmas

To design and analyze our algorithms, we present the following necessary lemmas.

Lemma 1 (see [34,37])**.** *Let* $V(\cdot) : \mathbb{R}_+ \to \mathbb{R}^{\mathrm{n}\times\mathrm{r}}$ *be regulated. Then,* $\dot{x} = \begin{bmatrix} -\mathrm{c}_1 VV^{\mathrm{T}} & I_n \\ -\mathrm{c}_2 VV^{\mathrm{T}} & 0 \end{bmatrix} x$ *is exponentially asymptotically stable iff* $V(\cdot)$ *is persistently exciting (PE), where* c_1 *and* c_2 *are positive constants.*

Lemma 2 (see [31])**.** *For the dynamic system*

$$\dot{\tilde{p}}_{i0}(t) = A_i(t)\tilde{p}_{i0} + f(t), \quad i \in \Omega, \tag{7}$$

where the coefficient matrix $A_i(t)$ *is continuous for all* $\mathrm{t} \in [0, \infty)$*, if constants* $r_i > 0$ *and* $b_i > 0$ *exist such that for every solution of the homogeneous differential equation* $\dot{\tilde{p}}_{i0}(t) = A_i(t)\tilde{p}_{i0}(t)$*, it holds that* $\|\tilde{p}_{i0}(t)\| \leq b_i \|\tilde{p}_{i0}(t_0)\| e^{-r_i(t-t_0)}$ *for* $0 \leq t_0 < t < \infty$*, then for all each* $f(t)$ *bounded and continuous on* $[0, \infty)$*, every solution of the nonhomogeneous Equation* (7) *is also bounded for* $t \in [0, \infty)$*. If* $\|f(t)\| \leq \varepsilon < \infty$*, then the solution of the perturbed system satisfies*

$$\left\|\tilde{p}_{i0}(t)\right\| \leq b_i \left\|\tilde{p}_{i0}(t_0)\right\| e^{-r_i(t-t_0)} + \frac{\varepsilon b_i^2}{r_i}(1 - e^{-r_i(t-t_0)}), \quad i \in \Omega. \tag{8}$$

3. Distributed Estimation and Circumnavigation Algorithms

To successfully estimate the relative target position p_{i0} and accomplish the control objectives described in Problem 1, an estimator $\hat{p}_{i0}$ and the control input (control protocol) u_i for each UAV are constructed as follows:

$$\dot{\hat{p}}_{io} = -\kappa_1 P_{\varphi_{io}} \hat{p}_{io} - \kappa_2 \int_0^{\mathrm{t}} P_{\varphi_{io}}(\tau)\hat{p}_{io}(\tau)\mathrm{d}\tau - \dot{p}_i, \quad i \in \Omega, \tag{9}$$

$$u_i = \gamma_1(\hat{D}_i - D^*)\varphi_{i0} + \gamma_2 D^*(\alpha + \gamma_3\Delta_i)\overline{\varphi}_{i0}, \quad i \in \Omega, \tag{10}$$

where κ_1, κ_2, γ_1, γ_2, γ_3 and α are positive design parameters, and $\hat{D}_i = \| \hat{p}_{i0} \|$ represents the estimated relative distance between the target and UAV i.

Remark 1. *In (9), the term $\dot{p}_i$ is equivalent to u_i in Equation (10), and is introduced to compensate for the estimation inaccuracies resulting from the movement of UAV i. The term $-\kappa_1 P_{\varphi_{io}} \hat{p}_{io} - \kappa_2 \int_0^{\mathrm{t}} P_{\varphi_{io}}(\tau)\hat{p}_{io}(\tau)\mathrm{d}\tau$ denotes the estimation of target velocity, structured as a PI controller. In (10), the radial term $\gamma_1(\hat{D}_i - D^*)\varphi_{i0}$ forces the agent to encircle the target with the desired distance D^*, while the tangential term $\gamma_2 D^*(\alpha + \gamma_3\Delta_i)\overline{\varphi}_{i0}$ ensures that the UAV rotate around the target while achieving the desired formation with other agents. In motion control, if D^* is set too small, the angular velocity of the UAV may become very large. To limit the angular velocity, the tangential term is adjusted to be dependent on D^*.*

We will first demonstrate that the estimation error $\tilde{p}_{i0}$ globally converges to a neighborhood of zero, leading to the following lemma.

Lemma 3. *Assuming that the estimation error $\tilde{p}_{i0}(0)$ in (3) is bounded, if the control parameters satisfy $\gamma_2 D^*\alpha - \varepsilon > \xi > 0$, where ξ is a given positive scalar, then the estimator (9) and control protocol (10) will cause $\tilde{p}_{i0}$ to exponentially converge to a circular area of radius $\frac{\varepsilon {b_i}^2}{r_i}$ centered at origin as $t \to \infty$, where r_i and b_i are defined in Lemma 2.*

Proof. Observing that $P_{\varphi_{i0}} p_{i0} = 0$, we can obtain

$$\begin{aligned} \dot{\tilde{p}}_{i0} &= \dot{\hat{p}}_{i0} - \dot{p}_{i0} \\ &= -\kappa_1 P_{\varphi_{i0}} \tilde{p}_{i0} - \kappa_2 \int_0^t P_{\varphi_{i0}}(\tau)\tilde{p}_{i0}(\tau)d\tau - \dot{p}_0, \quad i \in \Omega. \end{aligned} \tag{11}$$

Utilizing the property $P_{\varphi_{i0}} = \bar{\varphi}_{i0}\bar{\varphi}_{i0}^{\mathrm{T}}$ and defining $\varpi = -\kappa_2 \int_0^t P_{\varphi_{i_0}}(\tau)\tilde{p}_{i0}(\tau)d\tau$ as an auxiliary variable, Equation (10) can be rewritten as

$$\begin{bmatrix} \dot{\tilde{p}}_{i0} \\ \dot{\varpi} \end{bmatrix} = \begin{bmatrix} -\kappa_1 \overline{\varphi}_{i0}\overline{\varphi}_{i0}^{\mathrm{T}} & I \\ -\kappa_2 \overline{\varphi}_{i0}\overline{\varphi}_{i0}^{\mathrm{T}} & 0 \end{bmatrix} \begin{bmatrix} \tilde{p}_{i0} \\ \varpi \end{bmatrix} - \begin{bmatrix} \dot{p}_0 \\ 0 \end{bmatrix}, \quad i \in \Omega. \tag{12}$$

Obviously, System (12) can be divided into a nominal system

$$\begin{bmatrix} \dot{\tilde{p}}_{i0} \\ \dot{\varpi} \end{bmatrix} = \begin{bmatrix} -\kappa_1 \overline{\varphi}_{i0}\overline{\varphi}_{i0}^{\mathrm{T}} & I \\ -\kappa_2 \overline{\varphi}_{i0}\overline{\varphi}_{i0}^{\mathrm{T}} & 0 \end{bmatrix} \begin{bmatrix} \tilde{p}_{i0} \\ \varpi \end{bmatrix} \tag{13}$$

and a perturbation term $\begin{bmatrix} \dot{p}_0 \\ 0 \end{bmatrix}$. According to Lemma 2, if we can prove the global exponential stability of System (13), then we will be able to find some constants r_i and b_i such that Equation (8) holds, thereby proving Lemma 3. And by following Lemma 1, this objective can be redirected to prove that the unit vector $\bar{\varphi}_{i0}$ is persistently exciting.

It is known that if there exist $\varepsilon_{i1}, \varepsilon_{i2}, T_i > 0$ such that

$$\varepsilon_{i1} \leq \int_{t_0}^{t_0+T_i} \left(U^{\mathrm{T}} \overline{\varphi}_{i0}(\tau)\right)^2 d\tau \leq \varepsilon_{i2}, \quad i \in \Omega, \tag{14}$$

is satisfied for all unit constant vectors $U \in \mathbb{R}^2$ and all $t_0 > 0$, then $\bar{\varphi}_{i0}$ is PE (see [9]). Since $(U^{\mathrm{T}} \bar{\varphi}_{i0}(\tau))^2 \leq 1$, we can always find an upper bound $\varepsilon_{i2} = T_i$. Next, we shall prove that a lower bound ε_{i1} also exists. Let β_{Ui} be the angle measured counterclockwise from U to $\bar{\varphi}_{i0}$; its derivative is

$$\dot{\beta}_{Ui} = \frac{\gamma_2 D^*(\alpha + \gamma_3 \Delta_i) - \bar{\varphi}_{i0}{}^{\mathrm{T}} \dot{p}_0}{D_i}, \quad i \in \Omega. \tag{15}$$

Since $\| \ \bar{\varphi}_{i0}^{\mathrm{T}} \dot{p}_0 \ \| \leq \varepsilon$ and $\gamma_3 \Delta_i \geq 0$, we have $\gamma_2 D^*(\alpha + \gamma_3 \Delta_i) - \overline{\varphi}_{i0}{}^{\mathrm{T}} \dot{p}_0 > 0$. Therefore, if there exists an upper bound D_{imax} such that $D_i \leq D_{imax}$, then we can obtain $\dot{\beta}_{Ui} \geq \frac{\zeta}{D_{imcx}} > 0$; thus, one can always find a $\varepsilon_{i1} > 0$ and a $T_i > 0$ such that (14) is satisfied.

The final step is to show that D_i is indeed bounded. Defining $\tilde{D}_i = D_i - \hat{D}_i$, we derive the derivative of D_i:

$$\begin{aligned} \dot{D}_i &= \varphi_{i0}{}^{\mathrm{T}} (\dot{p}_0 - \dot{p}_i) \\ &= -\gamma_1 (D_i - D^*) + \gamma_1 \tilde{D}_i + \varphi_{i0}{}^{\mathrm{T}} \dot{p}_0, \quad i \in \Omega, \end{aligned} \tag{16}$$

and introducing the error $\delta_i = D_i - D^*$ between the distance of UAV i from the target and the desired distance results in

$$\delta_i = \delta_i(0) e^{-\gamma_1 t} + \int_0^t e^{-\gamma_1 (t-\tau)} (\gamma_1 \tilde{D}_i(\tau) + \varphi_{i0}^{\mathrm{T}}(\tau) \dot{p}_0(\tau)) d\tau, \quad i \in \Omega. \tag{17}$$

According to the triangular relationship, we have the following inequality:

$$\begin{aligned} |\tilde{D}_i(t)| &= | \ \| \ \hat{p}_{i0}(t) \ \| - \| \ p_{i0}(t) \ \| \ | \\ &\leq ||\hat{p}_{i0}(t) - p_{i0}(t)|| = ||\tilde{p}_{i0}(t)||, \quad i \in \Omega. \end{aligned} \tag{18}$$

Choose the Lyapunov candidate function $V = \frac{1}{2}(\tilde{p}_{i0}^{\mathrm{T}} \tilde{p}_{i0} + \varpi^{\mathrm{T}} \varpi)$. Given that the matrix $\begin{bmatrix} -\kappa_1 \overline{\varphi}_{i0} \overline{\varphi}_{i0}^{\mathrm{T}} & I \\ -\kappa_2 \overline{\varphi}_{i0} \overline{\varphi}_{i0}^{\mathrm{T}} & 0 \end{bmatrix}$ is negative semi-definite, we have $\dot{V} \leq 0$. This implies that the estimation error always remains $\tilde{p}_{i0}(t) \leq \tilde{p}_{i0}(0)$. Since $\tilde{p}_{i0}(0)$ is bounded, we can assume an upper bound ρ_i that satisfies $\tilde{p}_{i0}(t) \leq \rho_i$. Therefore, adding D^* on both sides of Equation (17), we can obtain

$$\begin{aligned} D_i(t) &\geq D^* + \delta_i(0) e^{-\gamma_1 t} - (1 - e^{-\gamma_1 t})(\rho_i + \frac{\varepsilon}{\gamma_1}), \\ D_i(t) &\leq D^* + \delta_i(0) e^{-\gamma_1 t} + (1 - e^{-\gamma_1 t})(\rho_i + \frac{\varepsilon}{\gamma_1}), \quad i \in \Omega. \end{aligned} \tag{19}$$

From (19), we can see D_i is bounded, and we have $D_{imax} = D^* + max\{\delta_i(0), \rho_i + \frac{\varepsilon}{\gamma_1}\}$. Hence, we have completed the proof of Lemma 3. □

Remark 2. *For a proportional-integral (PI) controller, the integral term prevents the error from growing indefinitely by capping it. Given that the target speed $\dot{p}_0$ has been regarded as a bounded disturbance, the estimation error $\| \ \tilde{p}_{i0}(t) \ \|$ will consequently remain bounded throughout the target estimation process. By integrating the error over time, the PI controller drives the error towards an acceptable range.*

Remark 3. *Based on (19), we can also determine a lower bound $D_{imin} \geq D^* - max\{\delta_i(0), \rho_i + \frac{\varepsilon}{\gamma_1}\}$ for D_i. This suggests that by reasonably setting the value of the desired radius D^*, we*

can ensure that $D_i(t) > 0$ for all $t \geq 0$, thereby guaranteeing UAV i can consistently obtain the bearing vector φ_{i0} while avoiding collisions between the UAVs and the target at all times.

Next, on the proof of Lemma 3, we will show that the distance error δ_i globally converges to a ball centered at zero for all the UAVs.

Theorem 1. *Under the estimation strategy (9), the controller (10) makes the relative distance D_i between the target and UAV i converge exponentially fast to a bounded circular area centered at D^* with radius $\varepsilon(\frac{1}{\gamma_1} + \frac{b_i^2}{r_i})$.*

Proof. From (17), and using the triangular inequality (18), we have

$$\mid \delta_i(t) \mid \leq \mid \delta_i(0) \mid e^{-\gamma_1 t} + \int_0^t e^{-\gamma_1(t-\tau)}(\gamma_1 \parallel \widetilde{p}_{i0}(\tau) \parallel + \mid \varphi_{i0}^{\mathrm{T}}(\tau)\dot{p}_0(\tau) \mid)d\tau, \quad i \in \Omega. \tag{20}$$

Using Inequality (8) in Lemma 2, (20) can be rewritten as

$$\begin{aligned} \mid \delta_i(t) \mid \leq & \mid \delta_i(0) \mid e^{-\gamma_1 t} + \frac{1}{\gamma_1}(1 - e^{-\gamma_1 t})\varepsilon \\ & + \gamma_1 e^{-\gamma_1 t} \int_0^t e^{\gamma_1 \tau}[b_i \parallel \tilde{p}_{i0}(0) \parallel e^{-r_i \tau} + \frac{\varepsilon b_i^2}{r_i}(1 - e^{-r_i \tau})]d\tau \\ \leq & \mid \delta_i(0) \mid e^{-\gamma_1 t} + \frac{1}{\gamma_1}(1 - e^{-\gamma_1 t})\varepsilon + \frac{\gamma_1 b_i(r_i \parallel \tilde{p}_{i0}(0) \parallel -\varepsilon b_i)}{r_i(\gamma_1 - r_i)}(e^{-r_i t} - e^{-\gamma_1 t}) \\ & + \frac{\varepsilon b_i^2}{r_i}(1 - e^{-\gamma_1 t}), \quad i \in \Omega, \end{aligned} \tag{21}$$

and letting $t \to \infty$, we finally obtain

$$\lim_{t \to \infty} \mid \delta_i(t) \mid \leq \varepsilon(\frac{1}{\gamma_1} + \frac{b_i^2}{r_i}), \quad i \in \Omega. \tag{22}$$

Therefore, as indicated by (22), the distance between the target and each UAV i converges to a neighborhood around the desired radius D^* as $t \to \infty$. □

Finally, we aim to demonstrate that the UAVs will arrange themselves in a regular polygon formation along the circumference of a circle, thereby achieving an optimal enclosing performance.

Theorem 2. *For all r_i and b_i, assume that the communication radius satisfies*

$$\rho \geq 2[D^* + \varepsilon(\frac{1}{\gamma_1} + \frac{b_i^2}{r_i})]. \tag{23}$$

Then, under estimator (9) and control law (10), each Δ_i converges exponentially to a bounded circular area centered at $\frac{2\pi}{\mathrm{n}}$.

Proof. According to Theorem 1, δ_i converges exponentially to a ball centered at zero with radius $\varepsilon(\frac{1}{\gamma_1} + \frac{b_i^2}{r_i})$. Therefore, under (23), there exists a time $0 < T_0 < \infty$ such that for all $t > T_0$, we have $N_i = \{1, \cdots, n\}/\{i\}$. This implies that each UAV i will always maintain a neighbor v_i, while simultaneously ensuring that $\sum_{i=1}^{n} \Delta_i = 2\pi$. Then, we calculate the derivative of Δ_i:

$$\begin{aligned}\dot{\Delta}_i &= \dot{\beta}_{U\nu_i} - \dot{\beta}_{Ui} \\ &= \frac{\gamma_2 D^*(\alpha+\gamma_3\Delta_{\nu_i}) - \bar{\varphi}_{\nu_i,0}^{\mathrm{T}}\dot{p}_0}{D_{\nu_i}} - \frac{\gamma_2 D^*(\alpha+\gamma_3\Delta_i) - \bar{\varphi}_{i0}^{\mathrm{T}}\dot{p}_0}{D_i} \\ &= \gamma_2\gamma_3(\Delta_{\nu_i}-\Delta_i) + \gamma_2\gamma_3(\frac{\Delta_i\delta_i}{D_i} - \frac{\Delta_{\nu_i}\delta_{\nu_i}}{D_{\nu_i}}) + \gamma_2 D^*\alpha(\frac{1}{D_{\nu_i}} - \frac{1}{D_i}) \\ &\quad + (\frac{\bar{\varphi}_{i0}}{D_i} - \frac{\bar{\varphi}_{\nu_i,0}}{D_{\nu_i}})^{\mathrm{T}}\dot{p}_0, \quad i \in \Omega.\end{aligned} \tag{24}$$

Define $\Delta = [\Delta_1, \cdots, \Delta_n]^{\mathrm{T}}$, and let $L(t)$ be the Laplacian matrix of the time-varying networked graph $G = (\Omega, E)$, where $E(t) = \{(\nu_i(t), i) : i \in \Omega\}$. We can rewrite Equation (24) as

$$\dot{\Delta}(t) = -\gamma_2\gamma_3 L(t)\Delta(t) + f_0(t) + f_1(t) + f_2(t), \tag{25}$$

where $[f_0(t)]_i = \gamma_2\gamma_3(\frac{\Delta_i\delta_i}{D_i} - \frac{\Delta_{\nu_i}\delta_{\nu_i}}{D_{\nu_i}})$, $[f_1(t)]_i = \gamma_2 D^*\alpha(\frac{1}{D_{\nu_i}} - \frac{1}{D_i})$, $[f_2(t)]_i = (\frac{\bar{\varphi}_{i0}}{D_i} - \frac{\bar{\varphi}_{\nu_i,0}}{D_{\nu_i}})^{\mathrm{T}}\dot{p}_0$ and $[L(t)]_{ij} = \begin{cases} 1 & j = i \\ -1 & j = \nu_i \\ 0 & otherwise \end{cases}$. Since G is a strongly connected graph, the $\Delta(t)$ in equation $\dot{\Delta}(t) = -\gamma_2\gamma_3 L(t)\Delta(t)$ will achieve consensus: $\Delta_i \to \frac{2\pi}{n}$. Thus, let $\tilde{\Delta} = [\Delta_1 - \frac{2\pi}{\mathrm{n}}, \cdots, \Delta_n - \frac{2\pi}{\mathrm{n}}]^{\mathrm{T}}$, and we can obtain

$$\dot{\tilde{\Delta}}(t) = -\gamma_2\gamma_3 L(t)\tilde{\Delta}(t) + f_0(t) + f_1(t) + f_2(t). \tag{26}$$

It is obvious that the disturbances $f_0(t)$, $f_1(t)$, $f_2(t)$ are bounded, and according to Lemma 2, the $\tilde{\Delta}$ will converge exponentially fast to a ball centered at zero. □

Based on Lemma 3, and Theorems 1 and 2, we have successfully achieved the estimation and control objectives (4)–(6). However, when the target's speed is high, the estimation error given by (9) and the control error for circumnavigation radius and interval angle given by (10) are unsatisfactory. Therefore, in the subsequent section of this paper, we will enhance our estimation and circumnavigation strategy by incorporating the Kalman filtering method to improve the encircling tracking performance.

4. Kalman Filtering Strategy

In this section, we will first utilize the local information exchange between neighboring UAV ν_i and UAV i to obtain an observation of the target's relative position. Then, by employing the Kalman filtering method, along with estimator (9), we can achieve a more accurate estimation of the target state, thereby improving the overall performance of collaborative target encircling tracking in the multi-UAV system.

As shown in Figure 1, when $N_i \neq \emptyset$, using trigonometric relationships, we have

$$D_i \mid sin\Delta_i \mid = D_{i,\nu_i} \mid sin\theta_{\nu_i,0} \mid, \quad i \in \Omega, \tag{27}$$

where $D_{i,\nu_i} = \parallel p_{i,\nu_i} \parallel$. By Lemma 5 in [38], for the angle $\theta \in [0, \pi]$ between any two unit vectors $x, y \in \mathbb{R}^2$, we have $sin\theta = \parallel P_x - P_y \parallel$. Thus, we can rewrite (27) as

$$D_i \parallel P_{\varphi_{i0}} - P_{\varphi_{\nu_i,0}} \parallel = D_{i,\nu_i} \parallel P_{\varphi_{i,\nu_i}} - P_{\varphi_{\nu_i,0}} \parallel, \quad i \in \Omega. \tag{28}$$

By calculating the derivative of φ_{i,ν_i}, we can obtain

$$\dot{\varphi}_{i,\nu_i} = \frac{P_{\varphi_{i,\nu_i}}(\dot{p}_{\nu_i} - \dot{p}_i)}{D_{i,\nu_i}}, \quad i \in \Omega. \tag{29}$$

In a practical environment, the values of φ_{i,ν_i} and $\dot{\varphi}_{i,\nu_i}$ can be measured directly by UAV i. Then, by substituting Equation (28), we can finally obtain $\hat{p}_{i0}^{observe}$ as the observation of the target's relative position for each UAV i:

$$\hat{p}_{i0}^{observe} = D_i \varphi_{i0} = \frac{\| P_{\varphi_{i,\nu_i}}(\dot{p}_{\nu_i} - \dot{p}_i) \|}{\| \dot{\varphi}_{i,\nu_i} \|} \frac{\| P_{\varphi_{i,\nu_i}} - P_{\varphi_{\nu_i,0}} \|}{\| P_{\varphi_{i,0}} - P_{\varphi_{\nu_i,0}} \|} \varphi_{i0}, \quad i \in \Omega. \tag{30}$$

Remark 4. *From Equations (27)–(30), we can easily see that the relative position observation* ${\hat{p}_{i0}}^{observe}$ *is calculated using the measurements of* φ_{i0}, φ_{i,ν_i}, *and their rate of change. In the theoretical analysis section, we do not consider the measurement noises for* φ_{i0}, φ_{i,ν_i}, *and their rates of change. However, the error of* ${\hat{p}_{i0}}^{observe}$ *can be affected by communication packet loss and bit errors between drones. We can model the observation noise as white Gaussian noise* $\vartheta(s)$ *with zero mean and covariance* $\mathbb{E}[\vartheta(s)\vartheta(t)] = \sigma_\vartheta^2 \delta(s-t)$, *where* $\delta(\cdot)$ *is a Dirac function and* σ_ϑ *is the standard deviation of the noise.*

By utilizing $\hat{p}_{i0}^{observe}$ with a Kalman filter, we can apply the following equations [39]:

$$\begin{aligned} \dot{X} &= AX + Bu + w, w \sim (0, Q) \\ Z &= HX + v, v \sim (0, R) \\ \widehat{X}(0) &= E[X(0)] \\ P(0) &= E[(X(0) - \widehat{X}(0))(X(0) - \widehat{X}(0))^{\mathrm{T}}], \\ K &= PH^{\mathrm{T}}R^{-1} \\ \dot{\widehat{X}} &= A\widehat{X} + Bu + K(Z - H\widehat{X}) \\ \dot{P} &= -PH^{\mathrm{T}}R^{-1}HP + AP + PA^{\mathrm{T}} + Q \end{aligned} \tag{31}$$

Here, X and Z represent the estimated and observed states of the target, determined by $[\hat{p}_{i0}, \dot{\hat{p}}_{i0}]^{\mathrm{T}}$ and $\hat{p}_{i0}^{observe}$, respectively. B and u represent the control input matrix and the control input. A and H are the state transition and observation models. The terms w and v denote process and measurement noises, following distributions $(0, Q)$ and $(0, R)$. Q and R are the covariance matrices of process and measurement noises. P represents the state covariance matrix, K is the Kalman gain factor, and $\widehat{X}$ denotes the estimated target state obtained through Kalman filtering.

Thus, we can improve the accuracy of the target state estimation in Equation (9) and obtain $\hat{X}_{i0}^{Kal} = [\hat{p}_{i0}^{Kal}, \hat{\dot{p}}_{i0}^{Kal}]^{\mathrm{T}}$ from $\widehat{X}$ in (31), where $\hat{p}_{i0}^{Kal}$ and $\hat{\dot{p}}_{i0}^{Kal}$ represent the relative position and relative velocity of the target after the Kalman filtering process. Then, by $\hat{p}_{i0}^{Kal}$, each UAV can estimate the global velocity of the target:

$$\hat{\dot{p}}_0^{Kal} = \dot{p}_i + \hat{\dot{p}}_{i0}^{Kal}, \quad i \in \Omega, \tag{32}$$

and by letting $\hat{D}_i^{Kal} = \| \hat{p}_{i0}^{Kal} \|$, we can modify the controller (10) by

$$\tilde{u}_i = \gamma_1(\hat{D}_i^{Kal} - D^*)\varphi_{i0} + \gamma_2 D^*(\alpha + \gamma_3 \Delta_i)\overline{\varphi}_{i0} + \hat{\dot{p}}_0^{Kal}, \quad i \in \Omega. \tag{33}$$

Remark 5. *The updated control law (33), in comparison to the preliminary controller (10), replaces* $\hat{D}_i$ *with* $\hat{D}_i^{Kal}$, *allowing agent i to employ more accurate relative distance estimation for achieving encirclement. Additionally, the additional term* $\hat{\dot{p}}_0^{Kal}$ *is introduced to compensate the circumnavigation error caused by the target's movement. If* $\hat{\dot{p}}_0^{Kal}$ *is similar to the actual target velocity, the problem can be treated as a static target circumnavigation problem.*

Theorem 3. *Through the estimated target state* $\hat{X}_{i0}^{Kal}$ *and the modified control law (33), when* $t \to \infty$, *we can finally obtain* $E[\tilde{p}_{i0}] = 0$, $E[\delta_i] = 0$ *and* $E[\Delta_i] = 0$.

Proof. Similar to the proof process of Corollary 1 and Corollary 2 in [16], based on Lemma 3, along with the unbiasedness of the Kalman filter, we can directly conclude that $E[\hat{X}_{i0}^{Kal} - X_{i0}] = 0$, for $i \in \Omega$. Here, $X_{i0} = [p_{i0}, \dot{p}_{i0}]^{\mathrm{T}}$ is the real state of the target. And from (32), we can also acquire

$$\begin{aligned} E[\hat{\dot{p}}_0^{Kal} - \dot{p}_0] &= E[\dot{p}_i + \dot{p}_{i0}^{Kal} - (\dot{p}_{i0} + \dot{p}_i)] \\ &= E[\dot{p}_{i0}^{Kal} - \dot{p}_{i0}] = 0, \quad i \in \Omega. \end{aligned} \tag{34}$$

Therefore, as $t \to \infty$, we have

$$\begin{aligned} E[\tilde{u}_i - \dot{p}_0] &= E[\gamma_1(\hat{D}_i^{Kal} - D^*)\varphi_{i0} + \gamma_2 D^*(\alpha + \gamma_3\Delta_i)\overline{\varphi}_{i0} + \hat{\dot{p}}_0^{Kal} - \dot{p}_0] \\ &= E[\gamma_1(\hat{D}_i^{Kal} - D^*)\varphi_{i0} + \gamma_2 D^*(\alpha + \gamma_3\Delta_i)\overline{\varphi}_{i0}] \\ &= \gamma_1(D_i^{Kal} - D^*)\varphi_{i0} + \gamma_2 D^*(\alpha + \gamma_3\Delta_i)\overline{\varphi}_{i0}, \quad i \in \Omega. \end{aligned} \tag{35}$$

Thus, the target tracking problem is transferred into the problem of encircling a static target, which means we can let $\varepsilon = 0$ in Inequality (22), and the disturbances $f_0(t)$, $f_1(t)$, and $f_2(t)$ in Equation (26) will finally vanish. That is, as $t \to \infty$, $E[\delta_i] = 0$ and $E[\Delta_i] = 0$. □

Remark 6. *In some cases, there may be situations where the observed value of $\hat{p}_{i0}^{observe}$ is lost. This can happen when $N_i = \emptyset$, or when the target, neighbor UAV, and UAV i are lined up in a straight line. In such situations, if the observed value is lost during the filtering process, we will use the estimated value $\hat{p}_{i0}$ instead of $\hat{p}_{i0}^{observe}$. This allows us to continue estimating the state of the target.*

At last, we demonstrate the implementation process of our algorithm.

Step 1: Define two integers, k and N, where k is the number of simulation steps, and N denotes a pre-set threshold value. Additionally, initialize the estimation of the relative target position $\hat{p}_{i0}$, the error covariance matrix P_k, prediction covariance matrix Q, and measurement covariance matrix R in the filter.

Step 2: When $k \leq N$, we estimate the target state using $[\hat{p}_{i0}, \hat{\dot{p}}_{i0}]^{\mathrm{T}}$ in Equation (9). Then, we update $\hat{\dot{p}}_{i0}^{Kal}$ as $-\kappa_1 P_{\varphi_{i0}}\hat{p}_{i0} - \kappa_2 \sum_{t_i=1}^{k} P_{\varphi_{i0}}(t_i)\hat{p}_{i0}(t_i)$, $\hat{D}_i^{Kal}$ as $\|\hat{p}_{i0}\|$ in control law (33). Finally, apply the updated control law to drive each UAV i.

Step 3: When $k > N$, we start the Kalman filtering process. Each UAV i begins to calculate $\hat{p}_{i0}^{observe}$ in Equation (30); if the observed value is not available, we let $\hat{p}_{i0}^{observe} = \hat{p}_{i0}$. Next, for agent i, by calculating $\hat{X}_{i0}^{Kal}$, we using the modified controller (33) to eventually complete the target encircling tracking.

5. Numerical Simulations

In this section, we will demonstrate several numerical examples to illustrate the theoretical results obtained in the previous sections.

Consider a formation of five circumnavigating UAVs and an unknown dynamic target in a GPS-denied indoor environment; the initial positions of the target and UAVs are assigned as $p_0 = [0, 0]^{\mathrm{T}}$, $p_1 = [-35, -40]^{\mathrm{T}}$, $p_2 = [36, -50]^{\mathrm{T}}$, $p_3 = [-2, -48]^{\mathrm{T}}$, $p_4 = [30, 49]^{\mathrm{T}}$ and $p_5 = [-26, 34]^{\mathrm{T}}$. The initial estimates of the relative target position are $\hat{p}_{10} = [-5, -15]^{\mathrm{T}}$, $\hat{p}_{20} = [31, -25]^{\mathrm{T}}$, $\hat{p}_{30} = [17, -36]^{\mathrm{T}}$, $\hat{p}_{40} = [5, 21]^{\mathrm{T}}$ and $\hat{p}_{50} = [-11, 27]^{\mathrm{T}}$. The desired circumnavigating radius is set as $D^* = 5$.

The designed parameters in Estimator (9) and Controller (10) are given as $\kappa_1 = 4$, $\kappa_2 = 0.12$, $\gamma_1 = 1.2$, $\gamma_2 = 1$, $\gamma_3 = 0.4$ and $\alpha = 1$. Let Δt represent the simulation step size, and set Δt to be 0.01 s. We define two different speed levels for the target: a velocity of $0.1v_t$ for low speed and a velocity of v_t for high speed, where $v_t = [2 - 2cos(0.1t), 2 + sin(0.05t)]^{\mathrm{T}}$.

We first assess the impact of the rough estimator (9) and control protocol (10) on tracking the low-speed target. The simulation results, as depicted in Figure 2, reveal that while the drones can maintain an accurate estimation of the target's relative position, the effectiveness of the circumnavigation is not satisfactory. It is evident from the results that, with only the rough distributed estimation and circumnavigation algorithm, the target state estimation ultimately converges to a neighborhood of the accurate value. The distance error δ_i between agent i and the target also converges to a neighborhood of zero, and the separation angle Δ_i between two neighboring UAVs converges to a neighborhood of the desired value $\frac{2\pi}{n}$. However, it is apparent that the results are not ideal, as the circumnavigation errors exhibit obvious fluctuations.

Now, we adopt the filtering strategy. We set $N = 2500$, and utilize the observed value $\hat{p}_{i0}^{observe}$ from Equation (30) and the modified control law (33). Additionally, let the state transition matrix $\Phi = \begin{bmatrix} 1 & \Delta t & (\frac{\Delta t}{2})^2 \\ 0 & 1 & \Delta t \\ 0 & 0 & 1 \end{bmatrix} \otimes I$ and the observation matrix $\overline{H} = \begin{bmatrix} 1 & 0 & 0 \end{bmatrix} \otimes I$, we select the following target dynamic model [40,41]:

$$\begin{aligned} X(k) &= [x(k) \quad u(k) \quad a(k)]^{\mathrm{T}}, \\ X(k) &= \Phi X(k-1) + w(k), \\ Z(k) &= \overline{H} X(k) + v(k), \end{aligned}$$

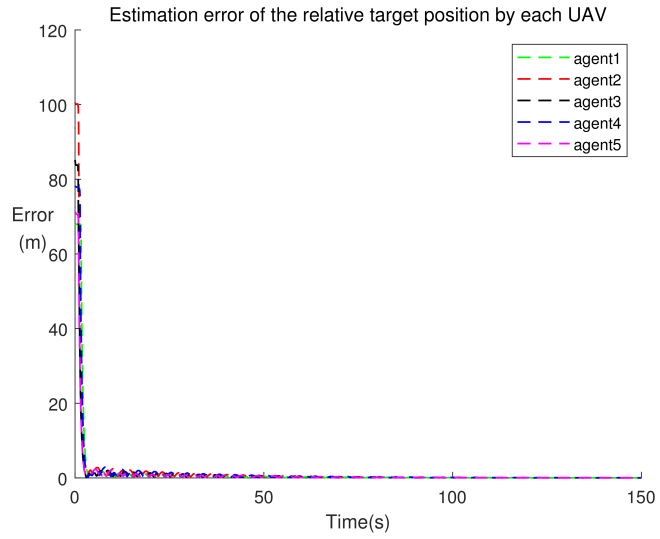
where the state vector $X(k)$ has a dimension of 6×1. The 2×1 vectors $x(k)$, $u(k)$, $a(k)$ refer to the target state variables to be estimated, respectively, representing the position, velocity, and acceleration in the k-th step of the simulation. $Z(k)$ represents the observed values of the target state. $w(k)$ and $v(k)$ represent process noise and measurement noise, respectively, assumed to be zero-mean Gaussian white noise. We set $P_k(0) = I_6$, $Q = 0.2I_6$ and $R = I$. The simulation results in low-speed target scenario are shown in Figure 3.

By comparing Figure 3 with Figure 2, we can observe that the application of the Kalman filter has further improved the accuracy of estimating the target's relative position and the circumnavigation control, enabling the multi-UAV system to accurately encircle and track the low-speed moving target.

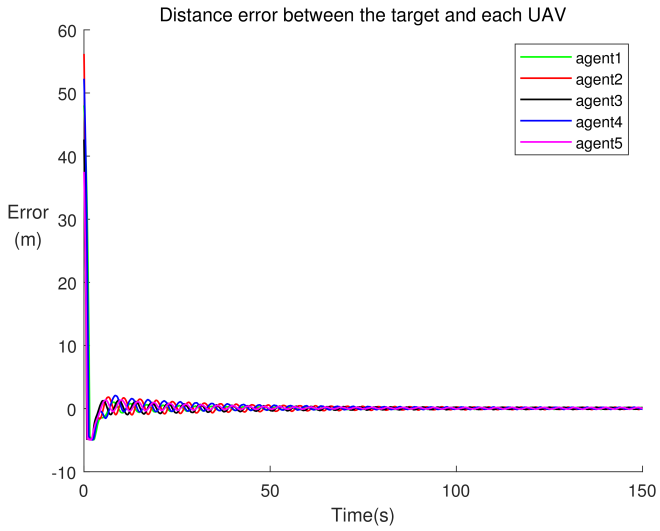
Then, we begin to discuss the high-speed scenario; the corresponding results are depicted in Figures 4–6. From these results, it can be seen that the system also performs well in circumnavigation tracking of high-speed moving targets. It is able to accurately estimate the target's state and execute the circumnavigation maneuvers precisely.

Considering the potential disturbance to the UAVs caused by air currents, which could lead to interference in bearing measurements, we conducted a simulation experiment. The simulation involved perturbing the bearing unit vectors φ_{i0} and φ_{ij} with Gaussian noise $n(\cdot)$. The noise follows $E[n(\cdot)] = 0$ and $E[n(t)n(s)] = 0.035\delta(t-s)$. The simulation results, as shown in Figure 7, indicate that the system still maintains satisfactory circumnavigation performance around the high-speed target, demonstrating a significant level of robustness against noise.

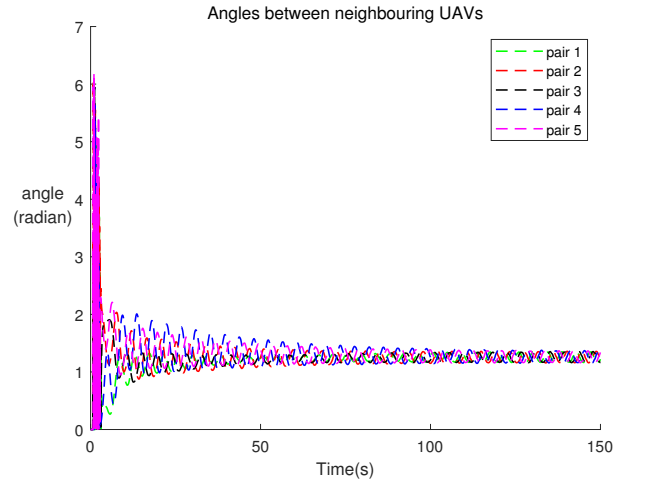
Finally, to substantiate the performance of our algorithm, we have conducted comparisons with the methods in reference [16,31]. In reference [16], the authors employed a single UAV equipped with GPS technology. They used the Virtual Intersecting Location Algorithm (VILA) to calculate a virtual observation value of the target state. Subsequently, by utilizing a Kalman filter and an initial estimation algorithm, the UAV estimated the target state and successfully accomplished the task of encircling the target. We selected the estimator (3) and the controller (17) from that reference, with the UAV's velocity v set to 20 and the estimation parameter k_E set to 200. The circumnavigation tracking results for both low-speed and high-speed targets are shown in Figure 8.



(**a**)

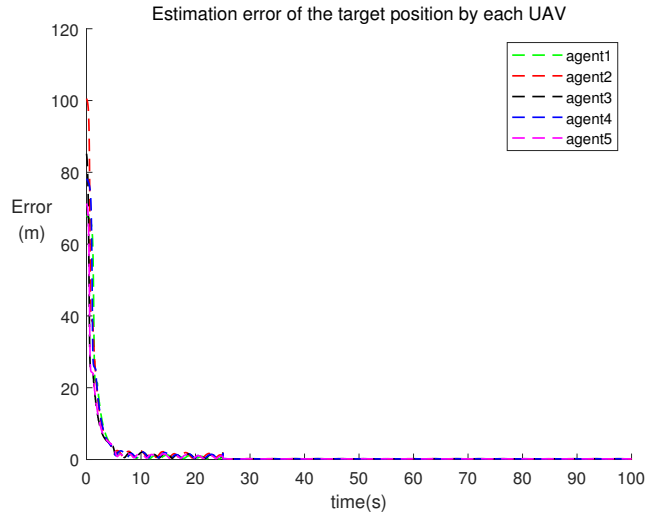


(**b**)

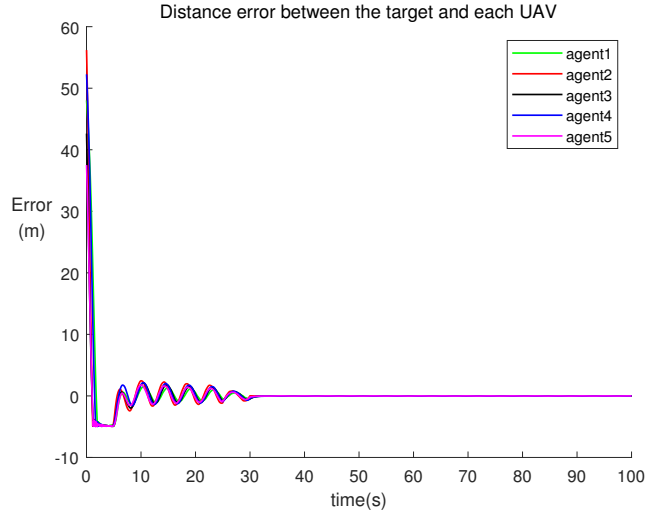


(**c**)

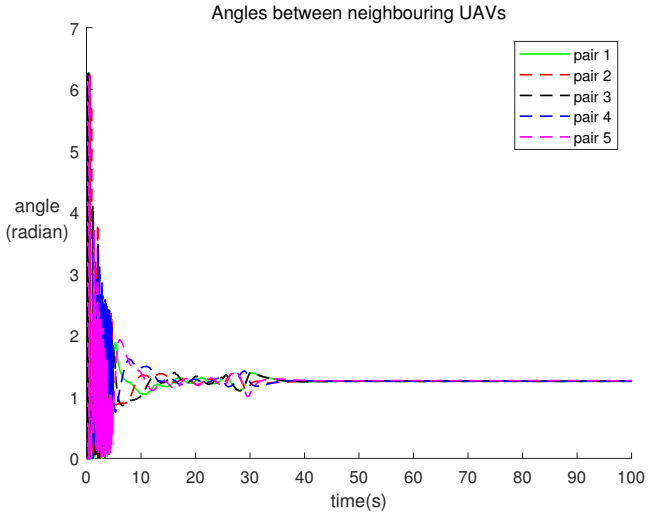
Figure 2. Estimation of relative position and encircling effect for the low-speed target using estimator (9) and control protocol (10). (**a**) Change of the relative target position estimation error $\| \hat{p}_{i0} - p_{i0} \|$. (**b**) Change in the circumnavigation radius controlling error $D_i - D^*$. (**c**) Change in the angles between neighboring UAVs.



(**a**)

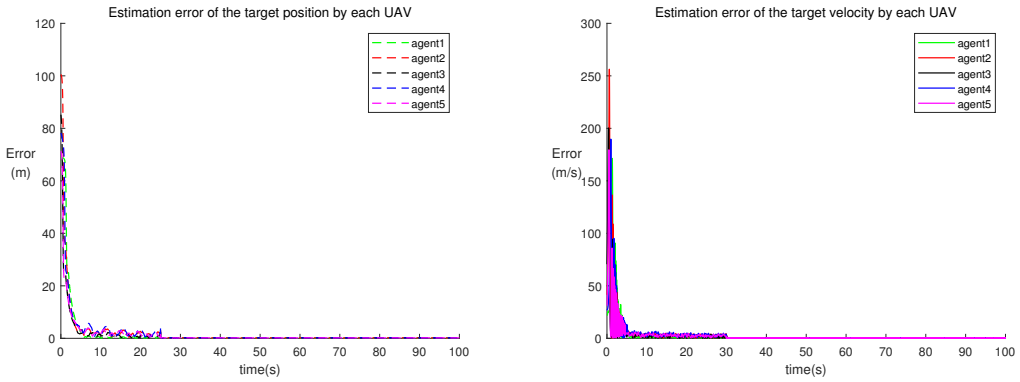


(**b**)



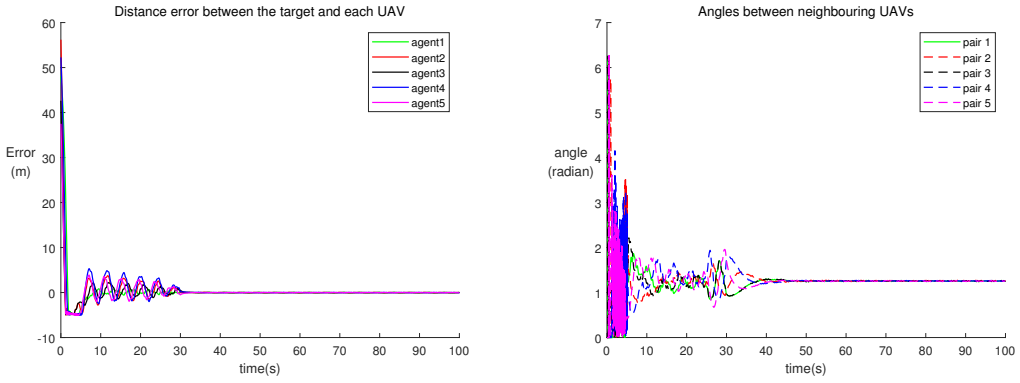
(**c**)

Figure 3. Estimation of relative position and encircling effect for the low-speed target by the Kalman filtering method. (**a**) Change of the relative target position estimation error $\| \hat{p}_{i0} - p_{i0} \|$. (**b**) Change in the circumnavigation radius controlling error $D_i - D^*$. (**c**) Change in the angles between neighboring UAVs.



(**a**) (**b**)

Figure 4. The impact of target state estimation by the Kalman filtering method in high-speed target scenario. (**a**) Change of the relative target position estimation error $\| \hat{p}_{i0}^{Kal} - p_{i0} \|$. (**b**) Change in the relative target velocity estimation error $\| \hat{p}_{0}^{Kal} - \dot{p}_{0} \|$.



(**a**) (**b**)

Figure 5. The target encircling tracking effect by the Kalman filtering method in high-speed target scenario. (**a**) Change of the circumnavigation radius controlling error $D_i - D^*$. (**b**) Change in the angles between neighboring UAVs.

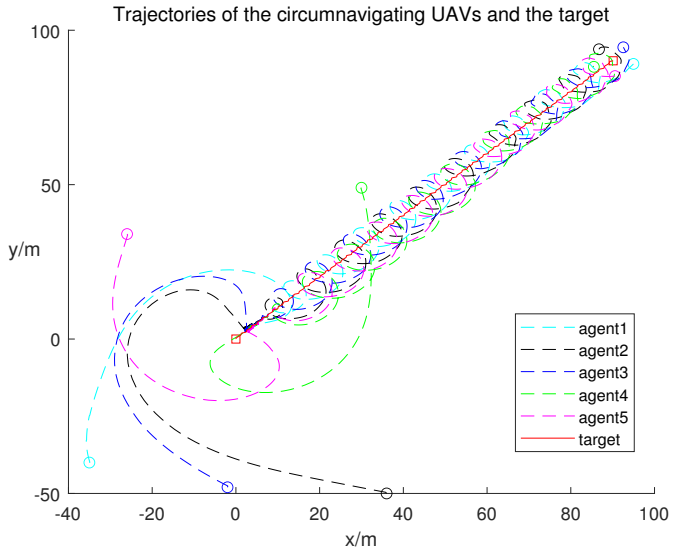
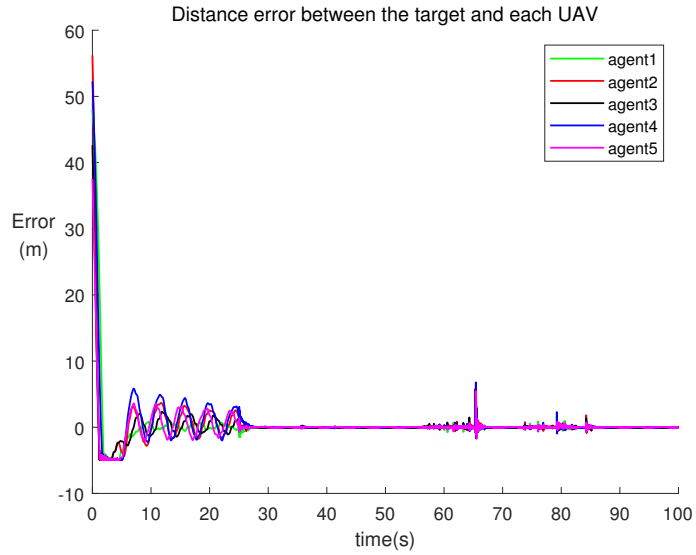


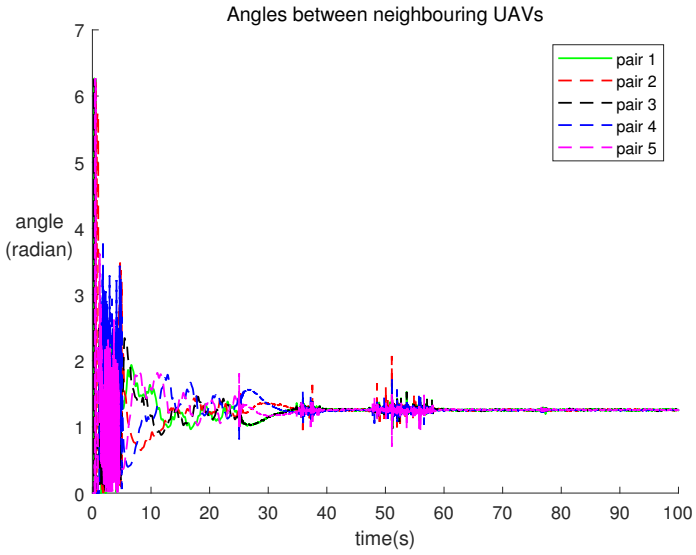
Figure 6. Trajectories of the target and circumnavigating UAVs during the encircling tracking process by the Kalman filtering method in the high-speed target scenario.

Additionally, in reference [31], the authors considered a scenario where five agents track a moving target in a GPS-denied environment. We adopted the estimation method (18) from that reference, and set the parameter k_i to 12. The initial states of all agents were adjusted to match our situation. The simulation results of the comparative analysis are depicted in Figure 9. For the high-speed target, simulated control indicators show significant deviations from their desired values. Therefore, corresponding simulation illustrations are not be presented here. It is evident that neither of the two existing methods can ensure accurate target encircling tracking when the target has a high speed.

Through Figures 8 and 9, it can be observed that existing typical algorithms can only successfully achieve encircling tracking in low-speed target scenario, while they perform poorly, or even fail, in encircling tracking of the high-speed target. By comparing with existing algorithms, the effectiveness of the algorithm designed in this paper is further validated.

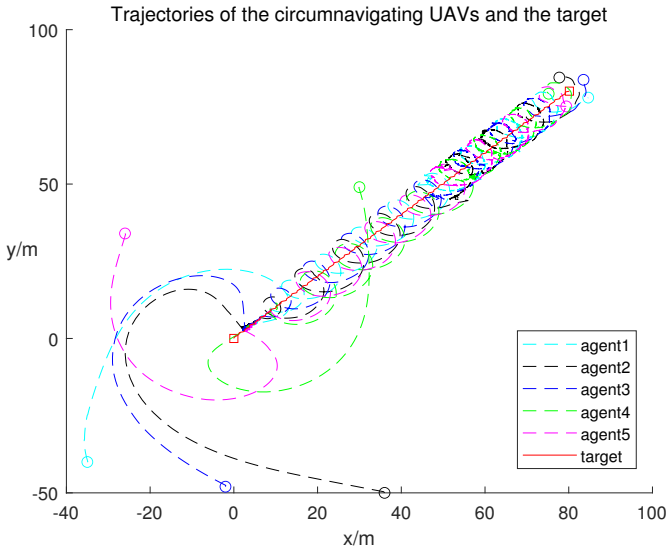


(**a**)



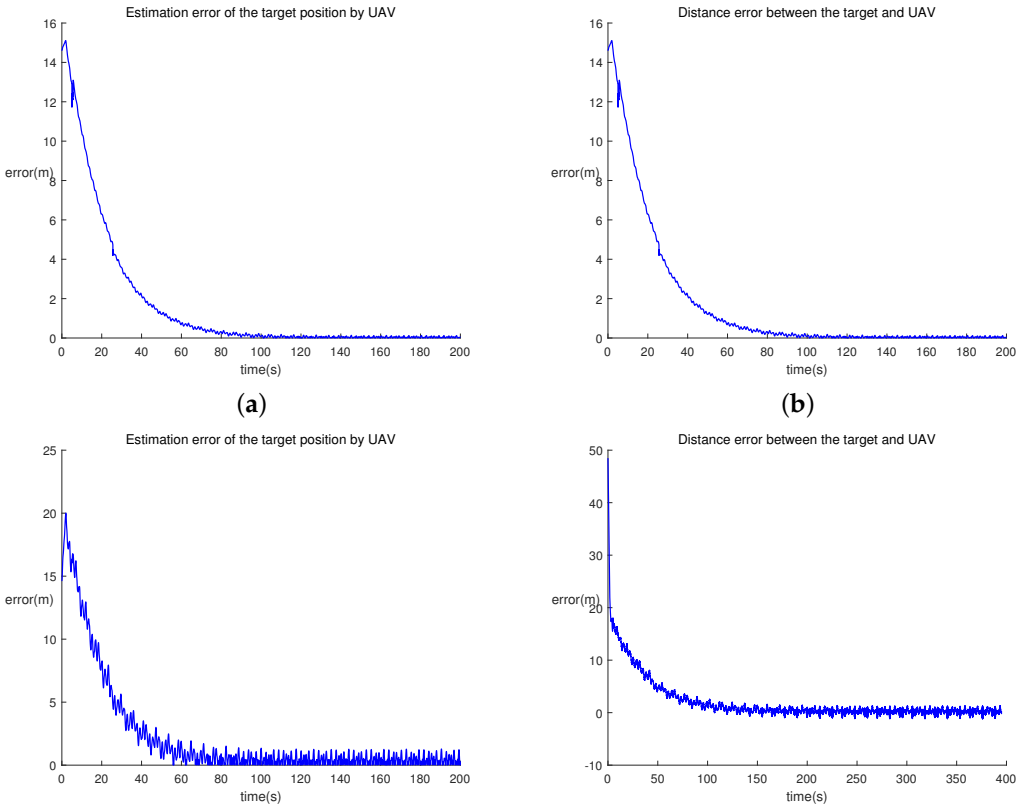
(**b**)

Figure 7. *Cont.*



(**c**)

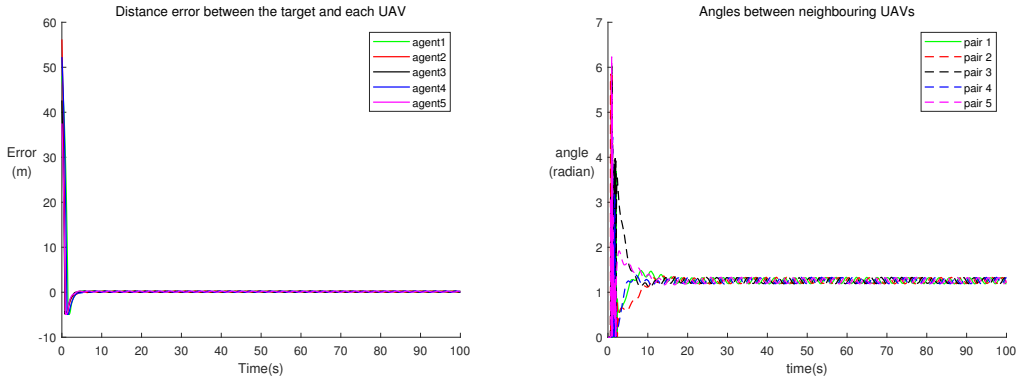
Figure 7. Target encircling tracking effect by the Kalman filtering method in the high-speed target scenario under noise disturbance. (**a**) Change of the circumnavigation radius controlling error $D_i - D^*$. (**b**) Change in the angles between neighboring UAVs. (**c**) Trajectories of the target and UAVs.



(**a**) (**b**)

(**c**) (**d**)

Figure 8. The target estimation and encircling effect by VILA method in the reference [16]. (**a**) Change of the target position estimation error $\| \hat{p}_0 - p_0 \|$ in low-speed target scenario. (**b**) Change in the circumnavigation radius controlling error $D_i - D^*$ in low-speed target scenario. (**c**) Change in the relative target position estimation error $\| \hat{p}_{i0} - p_{i0} \|$ in high-speed target scenario. (**d**) Change in the circumnavigation radius controlling error $D_i - D^*$ in high-speed target scenario.



(**a**) (**b**)

Figure 9. The circumnavigation effect of the method described in reference [31] for low-speed target in GPS-Free environment. (**a**) Change of the circumnavigation radius controlling error $D_i - D^*$. (**b**) Change in the angles between neighboring UAVs.

6. Conclusions

In this paper, we have developed a distributed estimation algorithm that utilizes bearing measurements of the target. Based on the estimated target state, we have designed a distributed circumnavigation control law to guide the UAVs to complete the mission of encircling the target. Moreover, we have leveraged the collaboration among UAVs by utilizing relative bearing and velocity information in the network to calculate relative positions of the target. Additionally, we incorporated a Kalman filtering strategy to refine our estimator and controller, thereby achieving more accurate target encircling tracking. In a future work, we will consider the high-speed target tracking problem for the case with more practice UAV dynamics in 3D space.

Author Contributions: Conceptualization, Z.Z., J.H. and B.C.; methodology, Z.Z. and J.H.; validation, Z.Z., B.C. and X.S.; investigation, Z.Z., J.H., B.C., X.S. and B.M.; writing—original draft preparation, Z.Z., B.C. and X.S.; writing—review and editing, Z.Z., J.H. and B.M. All authors have read and agreed to the published version of the manuscript.

Funding: This work was supported in part by the National Key Research and Development Program of China under Grant 2022YFE0133100, in part by the State Key Program of National Natural Science Foundation of China under Grant U21B2008, and in part by the Sichuan Science and Technology Program under Grant 2024NSFSC0528.

Data Availability Statement: The data used to support the findings of this study are available from the corresponding author upon request.

Conflicts of Interest: The authors declare no conflicts of interest.

References

1. Li, S.; Shao, X.; Zhang, W.; Zhang, Q. Distributed multicircular circumnavigation control for UAVs with desired angular spacing. *Def. Technol.* **2024**, *31*, 429–446. [CrossRef]
2. Chen, B.; Hu, J.; Ghosh, B.K. Finite-time tracking control of heterogeneous multi-AUV systems with partial measurements and intermittent communication. *Sci. China Inf. Sci.* **2024**, *67*, 152202. [CrossRef]
3. Chen, B.; Hu, J.; Zhao, Y.; Ghosh, B.K. Finite-time velocity-free rendezvous control of multiple AUV systems with intermittent communication. *IEEE Trans Syst. Man Cybern. Syst.* **2022**, *52*, 6618–6629. [CrossRef]
4. Chen, B.; Hu, J.; Zhao, Y.; Ghosh, B.K. Finite-time observer based tracking control of uncertain heterogeneous underwater vehicles using adaptive sliding mode approach. *Neurocomputing* **2022**, *481*, 322–332. [CrossRef]
5. Wang, R.; Shen, J. Disturbance observer and adaptive control for disturbance rejection of quadrotor: A survey. *Actuators* **2024**, *13*, 217. [CrossRef]
6. Lei, B.; Liu, B.; Wang, C. Robust geometric control for a quadrotor UAV with extended Kalman filter estimation. *Actuators* **2024**, *13*, 205. [CrossRef]
7. Duan, M.; Yang, Z.; Zhu, S.; Chen, C. Bearing-only containment control of multi-agent systems. *Int. J. Robust Nonlinear Control* **2023**, *33*, 11335–11350. [CrossRef]

8. Su, H.; Chen, C.; Yang, Z.; Zhu, S.; Guan, X. Bearing-based formation tracking control with time-varying velocity estimation. *IEEE Trans. Cybern.* **2023**, *53*, 3961–3973. [CrossRef]
9. Sewlia, M.; Zelazo, D. Bearing-based formation stabilization using event-triggered control. *Int. J. Robust Nonlinear Control* **2024**, *34*, 4375–4387. [CrossRef]
10. Mesbah, A. Stochastic model predictive control with active uncertainty learning: A survey on dual control. *Annu. Rev. Control* **2018**, *45*, 107–117. [CrossRef]
11. Deghat, M.; Shames, I.; Anderson, B.D.; Yu, C. Target localization and circumnavigation using bearing measurements in 2D. In Proceedings of the 49th IEEE Conference on Decision and Control, Atlanta, GA, USA, 5–17 December 2010; pp. 334–339.
12. Deghat, M.; Shames, I.; Anderson, B.D.; Yu, C. Localization and circumnavigation of a slowly moving target using bearing measurements. *IEEE Trans. Automat. Control* **2014**, *59*, 2182–2188. [CrossRef]
13. Deghat, M.; Xia, L.; Anderson, B.D.; Hong, Y. Multi-target localization and circumnavigation by a single agent using bearing measurements. *Int. J. Robust Nonlinear Control* **2015**, *25*, 2362–2374. [CrossRef]
14. Shao, J.; Tian, Y. Multi-target localisation and circumnavigation by a multi-agent system with bearing measurements in 2D space. *Int. J. Syst. Sci.* **2018**, *49*, 15–26. [CrossRef]
15. Li, R.; Shi, Y.; Wu, X.; Song, Y. Safe-circumnavigation of one single agent around a group of targets with only bearing information. *J. Frankl. Inst.* **2019**, *356*, 11546–11560. [CrossRef]
16. Qi, G.; Li, Y.; Sheng, A. Virtual intersecting location based UAV circumnavigation and bearings-only target-tracking techniques. *Inf. Sci.* **2019**, *505*, 571–585. [CrossRef]
17. Wang, W.; Chen, X.; Jia, J.; Fu, Z. Target localization and encirclement control for multi-UAVs with limited information. *IET Control Theory Appl.* **2022**, *16*, 1396–1404. [CrossRef]
18. Chen, K.; Qi, G.; Li, Y.; Sheng, A. Target localization and multicircular circumnavigation with bearing-only measurements. *Int. J. Adapt. Control Signal Process.* **2023**, *37*, 168–182. [CrossRef]
19. Chen, K.; Qi, G.; Li, Y.; Sheng, A. Finite-time target localization and multicircular circumnavigation with bearing-only measurements. *J. Frankl. Inst.* **2023**, *360*, 6338–6356. [CrossRef]
20. Ma, Z.; Li, Y.; Qi, G.; Sheng, A. Finite-time distributed localization and multi-orbit circumnavigation with bearing-only measurements. *J. Frankl. Inst.* **2023**, *360*, 6712–6735. [CrossRef]
21. Huang, S.; Teo, R.; Tan, K. Collision avoidance of multi unmanned aerial vehicles: A review. *Ann. Rev. Control* **2019**, *48*, 147–164. [CrossRef]
22. Niloy, M.; Shama, A.; Chakrabortty, R.; Ryan, M.; Badal, F.; Tasneem, Z. Critical design and control issues of indoor autonomous mobile robots: A review. *IEEE Access* **2021**, *9*, 35338–35370. [CrossRef]
23. Chen, K.; Qi, G.; Li, Y.; Sheng, A. Target Localization and Standoff Tracking with Discrete-Time Bearing-Only Measurements. *IEEE Trans. Circuits Syst. II Express Briefs* **2022**, *69*, 4448–4452. [CrossRef]
24. Chen, K.; Qi, G.; Li, Y.; Sheng, A. Cooperative localization and circumnavigation of multiple targets with bearing-only measurements. *J. Frankl. Inst.* **2023**, *360*, 9159–9179. [CrossRef]
25. Su, D.; Deghat, M. Communication-free bearing-only distributed target localization and circumnavigation by multiple agents. In Proceedings of the 2024 Australian and New Zealand Control Conference, Gold Coast, Australia, 1–2 February 2024; pp. 158–163.
26. Shao, X.; Li, S.; Zhang, J.; Zhang, F.; Zhang, W.; Zhang, Q. GPS-free collaborative elliptical circumnavigation control for multiple non-holonomic vehicles. *IEEE Trans. Intell. Veh.* **2023**, *8*, 3750–3761. [CrossRef]
27. Li, Z.; Tnunay, H.; Zhao, S.; Meng, W.; Xie, S.; Ding, Z. Bearing-only formation control with prespecified convergence time. *IEEE Trans. Cybern.* **2022**, *52*, 620–629. [CrossRef]
28. Wang, Z.; Chang, Y.; Zhang, H.; Yan, H. Bearing-only distributed localization for multi-agent systems with complex coordinates. *Inf. Sci.* **2023**, *626*, 837–850. [CrossRef]
29. Lin, Q.; Miao, Z.; Wang, Y.; Wu, Z.; He, W.; Fierro, R. Differentiator-based bearing-only formation control of quadrotors. *Int. J. Robust Nonlinear Control* **2023**, *33*, 10606–10624. [CrossRef]
30. Yu, Y.; Li, Z.; Wang, X.; Shen, L. Bearing-only circumnavigation control of the multi-agent system around a moving target. *IET Control Theory Appl.* **2019**, *13*, 2747–2757. [CrossRef]
31. Dou, L.; Song, C.; Wang, X.; Liu, L.; Feng, G. Target localization and enclosing control for networked mobile agents with bearing measurements. *Automatica* **2020**, *118*, 109022. [CrossRef]
32. Cao, S.; Li, R.; Shi, Y.; Song, Y. A low-cost estimator for target localization and circumnavigation using bearing measurements. *J. Frankl. Inst.* **2020**, *357*, 9654–9672. [CrossRef]
33. Cao, S.; Li, R.; Shi, Y.; Song, Y. Safe convex-circumnavigation of one agent around multiple targets using bearing-only measurements. *Automatica* **2021**, *134*, 109934. [CrossRef]
34. Hu, B.; Zhang, H. Bearing-only motional target-surrounding control for multiple unmanned surface vessels. *IEEE Trans. Ind. Electron.* **2022**, *69*, 3988–3997. [CrossRef]
35. Cao, S.; Duan, G. Bearing-only circumnavigation based on fully actuated system approach. In Proceedings of the 2nd Conference on Fully Actuated System Theory and Applications, Qingdao, China, 14–16 July 2023.
36. Kou, L.; Xiang, J. Target fencing control of multiple mobile robots using output feedback linearization. *Acta Autom. Sin.* **2022**, *48*, 1285–1291.
37. Sastry, S.; Bodson, M. *Adaptive Control: Stability, Convergence and Robustness*; Prentice-Hall: Chelmsford, UK, 2011.

38. Zhao, S.; Zelazo, D. Localizability and distributed protocols for bearing-based network localization in arbitrary dimensions. *Automatica* **2016**, *69*, 334–341. [CrossRef]
39. Bar-Shalom, Y.; Li, R.; Kirubarajan, T. *Estimation with Applications to Tracking and Navigation: Theory Algorithms and Software*; John Wiley and Sons: New York, NY, USA, 2001.
40. Wei, M.; Bar-Shalom, Y. Unbiased Kalman filter using converted measurements: Revisit. In Proceedings of the Signal and Data Processing of Small Targets 2009, San Diego, CA, USA, 2–6 August 2009.
41. Zhang, L.; Sidoti, D.; Bienkowski, A.; Pattipati, K.; Bar-Shalom, Y.; Kleinman, D. On the identification of noise covariances and adaptive Kalman filtering: A new look at a 50 year-old problem. *IEEE Access* **2020**, *8*, 59362–59388. [CrossRef]

Disclaimer/Publisher's Note: The statements, opinions and data contained in all publications are solely those of the individual author(s) and contributor(s) and not of MDPI and/or the editor(s). MDPI and/or the editor(s) disclaim responsibility for any injury to people or property resulting from any ideas, methods, instructions or products referred to in the content.